Control of Cavity Flow Based on a Macroscopic Observation

S. Djordjevic, P.M.J. Van den Hof, D. Jeltsema, R. van't Veen

Abstract— **A common approach to fluid flow modelling is based on a fine spatial discretization of the Navier-Stokes equations, which results in a large number of flow variables (i.e., microstates). For the purpose of flow control, the flow variables may be considered to be aggregated on a macroscopic level that goes beyond the fine modelling grid for a practical application. This paper addresses the problem of stabilizing fluid motions using a macroscopic variable that describes a flow pattern on a macroscopic level of observation. The results are illustrated using a lid driven cavity case in order to verify applicability of the macroscopic quantitative observation for a feedback control design.**

I. INTRODUCTION

Over the last few decades, control of fluid dynamics has become a problem of high interest in the control community [1]. This interest is due to the variety of industrial applications (e.g., transport of fluids in pipes, mixing of fluids in chemical reactors, air flow around wings). The goal of flow control, for a particular case, is to lower the operational expenses and improve the process performances. However, there is a number of complex issues underlying the problem of fluid motions that make the control problem extremely difficult to solve.

Generally, the motion of fluids can be described by using a set of nonlinear partial differential equations (PDEs), i.e., Navier-Stokes equations. To simulate the flow, the model equations are usually approximated by a large number of differential equations using specific discretization methods. The order of the spatially discretized model is determined by the discretization method and the number of discretization points. As the order of the system increases, the complexity of standard control issues like stability analysis, controllability and observability grows rapidly [2], [3], [4]. The literature presents three prototype flows with a simple geometry and different boundary conditions: plane channel flow (two periodic directions), pipe flow (one periodic direction) and cavity flow (no periodic direction). For the channel and pipe flow different control approaches have appeared, from linearized Navier-Stokes equations [5], [6], [7], [8], [9], [10], to more complex algorithms based on optimal control theory [11]. For the cavity flow, open-loop and closed-loop strategies are usually based on either reduced models or experiments [12], [13], [14], [15], since steady-state solutions can be obtained only numerically. For all geometries the actuation and flow sensing in the proposed algorithms require massive arrays of actuators and sensors embedded in a control system. Furthermore, the models based on the Navier-Stokes equations are coded using computational fluid dynamics (CFD) algorithms. It is well known that CFD is a rather difficult problem within simulation domains. Therefore, using the CFD codes for purposes of control design is a complex procedure which raises additional problems (e.g., input-output structure, numerical stability, simulation time). As these developments in flow control have partly been motivated by industrial applications, the implementation of the proposed controllers is still an open and challenging question. Recently, a global stabilization approach based on Lyapunov analysis of the system energetics has been explored for a channel flow [16], and a pipe [17]. The results show that the spatial changes in the control velocity are smooth and small, which suggests that in practice a small number of actuators can achieve the same goal [18], [19]. The analysis also indicates appropriate values of proportional feedback coefficients which enhance the $\mathcal{L}_2$ stability of the flow, whereas destabilization yields to an excellent result for mixing of fluid.

In most of this prior work, the flow variables are observed and controlled on a very detailed level, even though the variables may not be directly measurable. Since the problem of fluid motion basically lies in an enormous number of variables, the macroscopic observation of a specific flow problem can be rather beneficial for the practical implementation. In this paper, we introduce a macroscopic observation of fluid flow which can be obtained from the Navier-Stokes equations using an averaging method for a numerical experiment.

The paper is organized as follows. In Section II, we introduce the mathematical model of the lid driven cavity problem within an interconnected framework as a tool to design a macroscopic controlled variable. As a result, a general averaging procedure in the spatial domain is developed. Section III deals with the control design for the given problem. In Section IV, the control of the lid driven cavity case is presented to illustrate the procedure. Finally, Section V presents the conclusions and future works.

II. THE DYNAMICAL MODEL

As model equations, we consider the incompressible Navier-Stokes equations in two dimensional bounded space. A dimensionless form of the governing equations can be obtained by introducing dimensionless variables u and v as the velocity components in the x and y directions defined on

This work is supported by the Delft Center for Sustainable Industrial Processes.

S. Djordjevic, P.M.J. Van den Hof, R. van't Veen are with the Delft Center for Systems and Control, Delft University of Technology, Mekelweg 2, 2628 CD Delft, The Netherlands. s.djordjevic@tudelft.nl.

D. Jeltsema is with the Delft Institute of Applied Mathematics, Delft University of Technology, Mekelweg 4, 2628 CD Delft, The Netherlands. d.jeltsema@tudelft.nl.

ISBN 978-963-311-369-1

a rectangular domain $\Omega = [0,1] \times [0,1]$,

$$\frac{\partial u}{\partial x} + \frac{\partial v}{\partial y} = 0, \tag{1}$$

$$\frac{\partial u}{\partial t} = -u\frac{\partial u}{\partial x} - v\frac{\partial u}{\partial y} + \frac{1}{Re}\left(\frac{\partial^2 u}{\partial x^2} + \frac{\partial^2 u}{\partial y^2}\right) - \frac{\partial p}{\partial x}, \tag{2}$$

$$\frac{\partial v}{\partial t} = -u\frac{\partial v}{\partial x} - v\frac{\partial v}{\partial y} + \frac{1}{Re}\left(\frac{\partial^2 v}{\partial x^2} + \frac{\partial^2 v}{\partial y^2}\right) - \frac{\partial p}{\partial y}, \tag{3}$$

where p is the pressure and Re is the Reynolds number. The gravity effect and viscous dissipation outside the rectangular domain are neglected.

The initial conditions for the velocity field are zero, $u(t,x,y) = 0$, $v(t,x,y) = 0$ for $t = 0$. Boundary conditions for the velocity field are the velocity component in the x direction on top-wall (lid) and no-slip condition for velocity components at the bottom-wall and two sides walls,

$$\begin{aligned} u(t,x,1) &= \omega, & u(t,x,0) &= 0, \\ v(t,x,1) &= 0, & v(t,x,0) &= 0, \\ u(t,0,y) &= 0, & u(t,1,y) &= 0, \\ v(t,0,y) &= 0, & v(t,1,y) &= 0, \end{aligned}$$

where ω is the velocity of the lid. The geometry of the problem is illustrated in Fig.1.

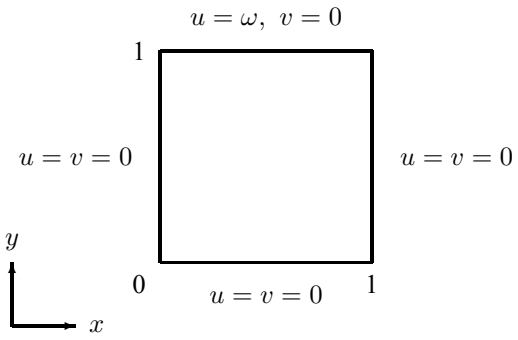

Fig. 1. Geometry of the lid driven cavity case.

The momentum equations (2) and (3) describe the time evolution of the velocity vector field (u, v) under inertial and viscous forces, whereas the pressure p is an implicit variable that satisfies the incompressibility condition (1). Since the incompressibility condition is not a time evolution equation but an algebraic condition, the pressure can be solved only by projecting the momentum equations onto the divergence-free velocity field [20]. From (1)-(3), it can be seen that the fluid motion is governed by implicit nonlinear PDEs, which requires complex numerical algorithms. The simulation results of the lid driven cavity case are given in Section IV.

A. Interconnected Form of a System

On a microscopic scale, the fluid motion can be described by solving model equations (1)-(3) using finite difference approximation. The PDE model is usually approximated with a large number of finite-dimensional differential equations

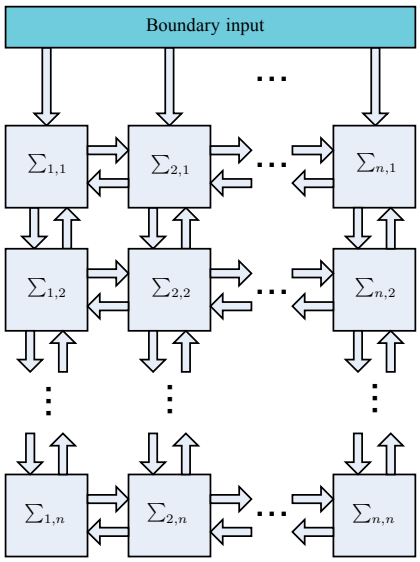

Fig. 2. Two dimensional interconnection of subsystems.

with algebraic constraints for the pressure correction. Based on the PDE model, the general form of the discretized model can be obtained introducing the state vector

$$z_{i,j} = \begin{bmatrix} u_{i,j} \\ v_{i,j} \end{bmatrix}, \tag{4}$$

where $i = 1, 2, ..., n$, $j = 1, 2, ..., n$ are the spatial indexes and $z_{i,j}$ is the state vector in $\mathbb{R}^{2n^2}$. Here the number of grid points in the x and y direction is chosen to be equal to n due to the simple geometry of the cavity case (see Fig. 1). This discretization method will result in a large number of nonlinear equations with algebraic constraints that can be represented in a general form as interconnection of subsystems $\sum_{i,j}$ with the following model equations

$$\begin{aligned} \dot{z}_{i,j} &= f_{i,j}(z_{i,j}, z_{i-1,j}, z_{i+1,j}, z_{i,j-1}, z_{i,j+1}, p_{i,j}) \\ &\quad + g_{i,j}(z_{i,j}, z_{i-1,j}, z_{i+1,j}, z_{i,j-1}, z_{i,j+1}, p_{i,j}) w_{i,j}, \end{aligned} \tag{5}$$

$$0 = \phi_{i,j}(z_{i,j}, z_{i-1,j}, z_{i+1,j}, z_{i,j-1}, z_{i,j+1}, p_{i,j}). \tag{6}$$

The indexes $i-1$, $i+1$, $j-1$ and $j+1$ are complementary indexes, and they illustrate the way the subsystems are coupled [22]. Functions $f_{i,j}$ and $\phi_{i,j}$ are smooth functions that approximate the time evolution of the velocity field (2)-(3) and the constraint equation (1), respectively. The boundary input $w_{i,j}$ is considered to be the velocity vector of the top-wall (see Fig. 2)

$$w_{i,1} = \begin{bmatrix} u_{i,1} \\ v_{i,1} \end{bmatrix} = \begin{bmatrix} \omega \\ 0 \end{bmatrix}.$$

The idea is that (5)-(6) can be seen as a system consisting of n^2 subsystems $\sum_{i,j}$ that are interconnected by complementary state vectors, $z_{i-1,j}$, $z_{i+1,j}$, $z_{i,j-1}$ and $z_{i,j+1}$, to the systems $\sum_{i-1,j}$, $\sum_{i+1,j}$, $\sum_{i,j-1}$ and $\sum_{i,j+1}$, respectively. In this way, the stability analysis of the interconnected system reduces to the stability problem of the subsystems, whereas the controllability and observability of the interconnected

system reduces to the complementary state vectors. When a system contains many states which can be controlled and measured, the measurable variables have to be chosen such that the overall system can be evaluated. For this reason, we will, instead of observing the microstates $z_{i,j}$ in the domain Ω, introduce a macroscopic domain over which the controlled variable is defined, i.e.,

$$\overline{\Omega}_{k,k} = \Delta x_k \Delta y_k, \qquad k = 1, 2, ..., r,$$

where $\overline{(\cdot)}$ indicates the macroscopic quantitative observation. The index k is a macroscopic observation index which specifies the macroscopic domain. Note that the macroscopic space is much smaller than the microscopic one, i.e., $r \ll n$. The number of grid points in the x and y direction for the macroscopic space is equal to r. The state values of the velocity field from the microscopic model presented in (1)-(3) are the basis for deriving the macroscopic controlled variable

$$y_{k,k} = \frac{1}{\overline{\Omega}_{k,k}} \sum_{i=\frac{(k-1)}{r}n+1}^{\frac{k}{r}n} \sum_{j=\frac{(k-1)}{r}n+1}^{\frac{k}{r}n} h_{i,j}(z_{i,j}), \qquad (7)$$

where $y_{k,k}$ is the output in $\mathbb{R}^{r^2}$. Here an averaging approach is considered as the mapping between the microstates derived in (5)-(6) and macrostates as the controlled variables, although other relations can be used as well. In principle, the procedure is applicable to systems where the changes in the microstates of each subsystem are small and bounded in time.

B. Macroscopic Averaging of Fluid Motion

As is shown in the previous section, the fluid motion is described by the velocity field with components in the x and y direction. The system is fully driven by the lid velocity $w_{i,1}$. Since the velocity components are also vectors, we aim for a scalar function that can represent the flow patterns. In general, the work done by the boundary input influences the velocity and, consequently, influences the energy distribution over the domain Ω. The system considered in this paper is an incompressible fluid with no heat exchange; therefore, the rate of energy changes over the rectangular domain Ω is proportional to the kinetic energy of the subsystems

$$E_{i,j} = \frac{1}{2}(u_{i,j}^2 + v_{i,j}^2) = \frac{1}{2}\|z_{i,j}\|_{\mathcal{L}_2}^2. \qquad (8)$$

In this way, we can obtain the macroscopic variables from (8) using the averaging procedure given in (7). The macroscopic variables in domain $\overline{\Omega}_{k,k}$ equal

$$\begin{aligned}\overline{E}_{k,k} &= \frac{1}{\overline{\Omega}_{k,k}} \sum_{i=\frac{(k-1)}{r}n+1}^{\frac{k}{r}n} \sum_{j=\frac{(k-1)}{r}n+1}^{\frac{k}{r}n} E_{i,j} \qquad (9)\\ &= (\overline{u_{k,k}^2} + \overline{v_{k,k}^2}).\end{aligned}$$

The fact that the energy is bounded in time for the given initial and boundary conditions can be used for assigning equilibrium points for the control design. The equilibrium points can be seen as desired outputs on a macroscopic level of observation.

III. CONTROL DESIGN

As a result of the analysis in the previous section, we will focus only on stable reference trajectories as a control objective. The boundary actuation implies several specific flow dynamics in the spatial domain Ω. These flows are considered as stable laminar flows for low Re or unstable for high Re. The unstable flows are characterized by the fact that small fluctuations from the steady velocity profile grow and, eventually, cause instability of the velocity profile.

For the system given in Section II, our control objective is to find a boundary control $w_{i,1}$ such that the error defined by

$$e_{k,k} = y_{k,k} - y_{k,k}^d \qquad (10)$$

converges to zero. The desired trajectory $y_{k,k}^d$ can be obtained from the macroscopic system analysis. Suppose that the system (5)-(6) is actuated with a specific constant input $w_{i,1}^*$. The system will have a certain response to the input. If the states $z_{i,j}(t)$ approach constant values when t goes to infinity, then $z_{i,j}^*(\infty)$ can be consider as a steady-state response of the system for the given input [23]. Consequently, the reference output trajectory will also approach a constant value, i.e.,

$$y_{k,k}^d = \frac{1}{\overline{\Omega}_{k,k}} \sum_{i=\frac{(k-1)}{r}n+1}^{\frac{k}{r}n} \sum_{j=\frac{(k-1)}{r}n+1}^{\frac{k}{r}n} h_{i,j}(z_{i,j}^*(\infty)) = const.$$

Now, we can pose the problem as finding a controller that maintain the desired output $y_{k,k}^d$ produced by the model under the effect of $w_{i,1}^*$. Note that the boundary input $w_{i,1}$ can have only one value ω since the lid can have only one velocity component in the x direction (see Fig. 1). The output feedback controller that achieves the control objective (10) is given as a PI controller

$$w_{k,1} = K_{k,k}^P(y_{k,k} - y_{k,k}^d) + K_{k,k}^I \xi_{k,k}, \qquad (11)$$

$$\dot{\xi}_{k,k} = y_{k,k} - y_{k,k}^d, \qquad (12)$$

where $K_{k,k}^P$ and $K_{k,k}^I$ are control parameters that can be tuned. The feedback control law should drive the system output towards the desired point with arbitrary fast exponential decay. The numerical results of tuning the control parameters are given in the next section.

IV. NUMERICAL EXAMPLE

In this section, the proposed output feedback strategy is demonstrated on the Navier-Stokes equations using four equally distributed spatial domains as a macroscopic observation $\overline{\Omega}_{k,k}$, where $k = 1, 2$ (see Fig. 3). We use a simple numerical method to solve the Navier-Stokes equations that is coded in Matlab [20], [21]. To improve numerical stability, the viscous term, which is a linear part of (2)-(3), is treated implicitly; and the convective term, which is a nonlinear part of (2)-(3), is treated explicitly. The momentum equations are first solved by neglecting the pressure term and then projecting them onto the subspace of the divergence-free velocity field. Equations (1)-(3) are discretized on 64×64 grid points in the spatial domain. Fig. 3 shows the simulation

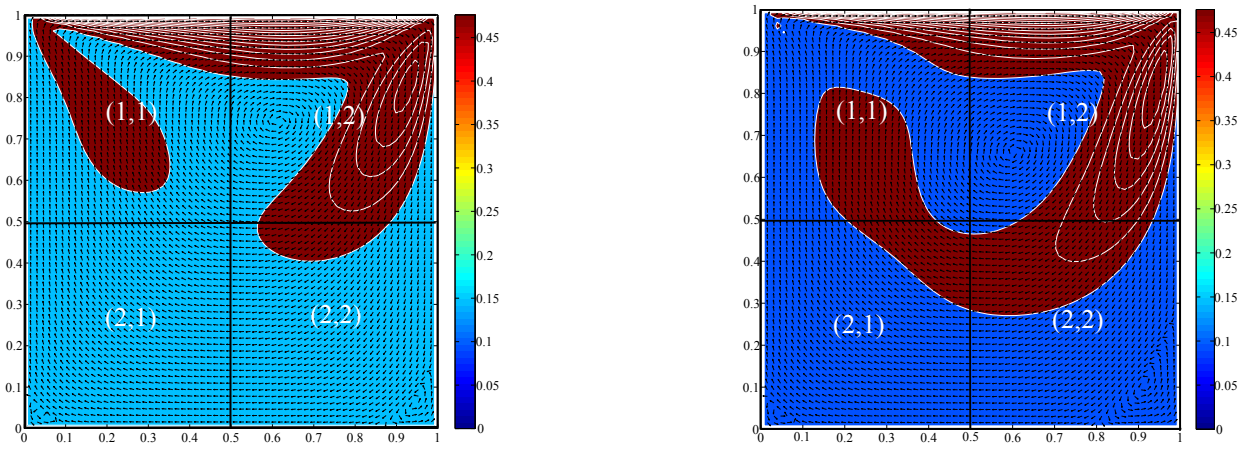

Fig. 3. Energy distribution $E_{i,j}$ in $\Omega_{i,j}$ and macroscopic space $\overline{\Omega}_{k,k}$ where $k = 1, 2$ at $t = 25$ for $Re = 100$ (left) and $Re = 250$ (right).

results of the energy distribution for two different Reynolds numbers: $Re = 100$ and $Re = 250$ at $t = 25$. As can be seen from Fig. 3, the flow is characterized by the primary dominance of a clockwise rotating subspace. This subspace is adjoined with two counterclockwise secondary rotating subspaces at the corners of the bottom-wall. The differences in energy levels over the entire space $\Omega_{i,j}$ are caused by the boundary input $\omega_{i,1} = \begin{bmatrix} 1 \\ 0 \end{bmatrix}$, initial conditions and Re. For the given boundary conditions, the energy level decreases in the whole space $\Omega_{i,j}$ starting from the top-wall to the bottom-wall. By increasing Re, the bottom vortexes become bigger and new vortexes can appear in left top corner.

Following the theoretical framework previously developed, the space $\Omega_{i,j}$ is divided into four macroscopic spaces $\overline{\Omega}_{k,k}$. These macroscopic spaces are then used for the control design. First, the equilibrium-like profile is evaluated from the energy level $\overline{E}_{k,k}$ in each subspace $\overline{\Omega}_{k,k}$ over the time domain which is illustrated in Fig. 4 and defined by (9). As expected, for low Re the energy level of each subspace approaches constant values when time increases. The macroscopic energy trajectories of each subspace $\overline{\Omega}_{k,k}$ show stable responses with respect to time and a macroscopic flow behaviour under influence of the boundary input. The considerable influence of the boundary input is noticed in $\overline{\Omega}_{2,1}$ and $\overline{\Omega}_{2,2}$, where the secondary vortex enlarges by increasing the boundary input. Therefore, the macroscopic energy level of $\overline{\Omega}_{2,2}$, which corresponds to the constant values, is considered to be the controlled variable. The desired macroscopic point $y^d_{2,2}$ for $Re = 100$ is 0.0081 and for $Re = 250$ is 0.0152, as illustrated in Fig. 4. After $y^d_{2,2}$ is determined, the parameters $K^P_{2,2}$ and $K^I_{2,2}$ can be tuned to enhance the asymptotic output regulation for the chosen macroscopic space, i.e., $\lim_{t\to\infty} h_{2,2}(z_{i,j}) = \overline{E}^d_{2,2}$ and $\lim_{t\to\infty} e_{2,2} = 0$.

First, we started by considering pure proportional feedback $K^P_{2,2}$ action at different gain settings. The effectiveness of the closed-loop system achieved by tuning the control parameters (11)-(12) is shown in Fig. 5 for $Re = 100$ and Fig. 6

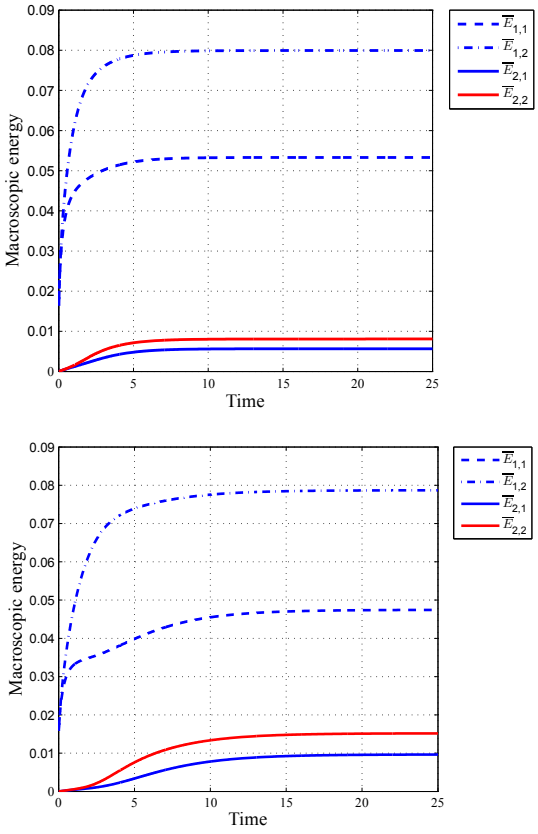

Fig. 4. Time evolution of $\overline{E}_{i,j}$ in $\overline{\Omega}_{k,k}$ domain for $Re = 100$ (top), and $Re = 250$ (bottom).

for $Re = 250$. By increasing the $K^P_{2,2}$, the error $e_{k,k}$ decreased but did not approach zero. Furthermore, it was observed that applying a high gain leads to flow instability and transition regimes that need longer time to be stabilized by the controller. To avoid this problem, we introduced the second control parameter $K^I_{2,2}$ which integrates the steady-state error and insures the zero steady-state error. For small

values of $K^I_{2,2}$, the observed macroscopic energy level moves towards the reference level, whereas for larger values of $K^I_{2,2}$, the error approaches zero with a small bounded oscillation. At the end, satisfactory output regulation is guaranteed with the control parameters given in Table I.

TABLE I

CONTROL PARAMETERS FOR REGULATION OF ENERGY LEVEL IN $\overline{\Omega}_{2,2}$

Re	$\overline{E}_{2,2}$	$K^P_{2,2}$	$K^I_{2,2}$
100	0.0081	100	62
250	0.0152	60	21

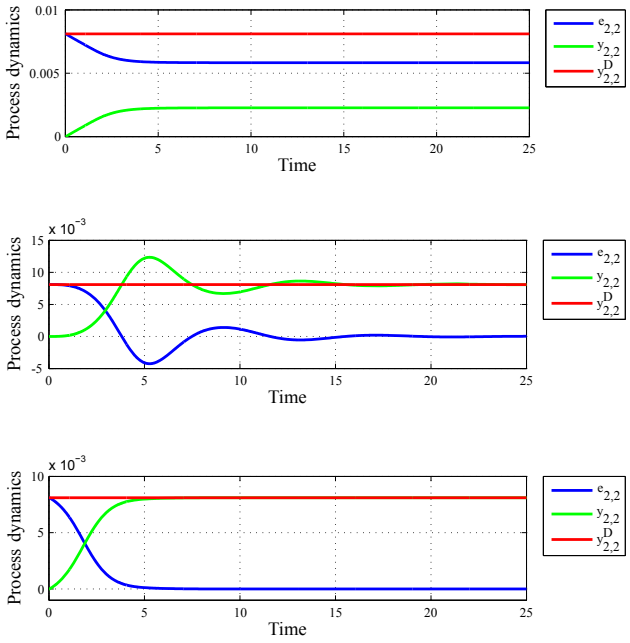

Fig. 5. Feedback control of the lid driven cavity case for $Re = 100$ with the control parameter $K^P_{2,2} = 100$ (top), $K^I_{2,2} = 62$ (centre), and $K^P_{2,2} = 100$ and $K^I_{2,2} = 62$ (bottom).

The simulation results show that the structure of the control laws predicted by the design can be used for flow regulation at steady-state for $Re = 100$ and $Re = 250$. For lager Re, the macroscopic energy trajectories show unstable responses due to numerical instability and turbulent effects. The direct numerical simulations (DNS) used in this example can not capture important dynamic of turbulent flows. Flows with high Re are usually modeled by means of velocity vectors and turbulent fluctuation. The mean velocities are independent of time when the mean flow is steady, whereas the fluctuations can have random nature. Since the mean flows are usually stable, it can be seen as a macroscopic controlled variable in this framework of flow control for turbulence models.

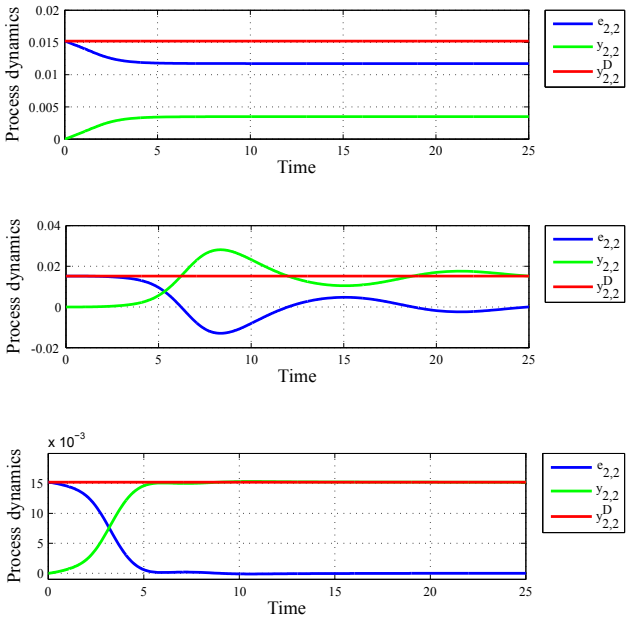

Fig. 6. Feedback control of the lid driven cavity case for $Re = 250$ with the control parameter $K^P_{2,2} = 60$ (top), $K^I_{2,2} = 21$ (centre), and $K^P_{2,2} = 60$ and $K^I_{2,2} = 21$ (bottom).

V. CONCLUSIONS AND FUTURE WORKS

A. Conclusions

In this paper, we have presented a simple design method by which is possible to regulate a flow via output feedback using a macroscopic controlled variable. Although the macroscopic observation does not contain the detailed information about the fluid motion, it can be seen as a controlled variable for a particular application which requires lower level of observation (e.g., thermodynamics in reactors). We have shown that the complexity of the control design in fluid flows can be considerably reduced by accounting different observation levels. The chosen control objective is a first attempt to control flows using macroscopic variables which can be extended for different flow cases.

B. Future Works

For the further development of the framework, the steady state analysis of flows with high Re should be investigated. This analysis requires an extensive algorithm that can modeled the transition effect of fluid flows. Improving the algorithm, the wide range of Re can be examined. Furthermore, for the particular application of fluid dynamics, it will be interesting to examine the size of macroscopic space sufficient for a control design, i.e., $\overline{\Omega}_{k,k}$ where $k = 1, 2, ..., r$ and $2 < r < n$.

REFERENCES

[1] T.R. Bewley, Flow control: new challenges for a new Renaissance, *Progress in Aerospace Sciences*, vol. 37, 2001, pp 21-58.

[2] J.-M. Coron, On the controllability of the 2D incompressible Navier-Stokes equations with the Navier slip boundary conditions, *ESAIM: Control, Optim. Cal. Var.*, vol. 1, 1996, pp 35-75.

[3] C. Fabre, Uniqueness results for Stokes equations and their consequences in linear and nonlinear control problems, *ESAIM: Control, Optim. Cal. Var.*, vol. 1, 1996, pp 267-302.
[4] O.Y. Imanuvilov, On exact controllability for the Navier-Stokes equation, *ESAIM: Control, Optim. Cal. Var.*, vol. 3, 1998, pp 97-131.
[5] S.S. Joshi, J.L. Speyer and J. Kim, A systems theory approach to the feedback stabilization of infinitesimal and finite-amplitude disturbances in plane Poiseuille flow, *J. Fluid Mech.*, vol. 332, 1997, pp 157-184.
[6] S.S. Joshi, J.L. Speyer and J. Kim, Finite-dimensional optimal control of poiseuille flow, *Journal of Guidance, Control, and Dynamics*, vol. 22, 1999, pp 340-348.
[7] L. Cortelezzi, K.H. Lee, J. Kim and J.L. Speyer, Skin-friction drag reduction via robust reduced-order linear feedback control, *Int. J. Comput. Fluid Dyn.*, vol.11, 1998, pp 79-92.
[8] L. Cortelezzi and J.L. Speyer, Robust reduced-order controller of laminar boundary layer transitions, *Phisical Review E*, vol. 58, 1998
[9] S.M. Kang, V. Ryder, L. Cortelezzi and J.L. Speyer, State-space formulation and controller design for three-dimensional channel flows, *Proceedings of the 1999 American Control Conference, San Diego, California*, 1999
[10] M.R. Jovanovic and B. Bamieh, Frequency domain analysis of the linearized Navier-Stokes equations, *Proceedings of the 2003 American Control Conference, Denver, Colorado*, 2003.
[11] T.R. Bewley, P. Moin and R. Temam, DNS-based predictive control of turbulence: an optimal benchmark for feedback algorithms, *J. Fluid Mech.*, vol. 447, 2001, pp 179-225.
[12] C.W. Rolweya and V. Juttijudata, Model-based control and estimation of cavity flow oscillations, *Proceedings of the 44th IEEE Conference on Decision and Control, and the European Control Conference 2005*, Seville, Spain, 2005.
[13] L.N. Cattafesta, III, S. Garg, M. Choudhari, and F. Li, Reviw of active control of flow-induced cavity resonance, AIAA Paper 97-1804, 2003.
[14] C.W. Rowley, T. Colonius, and A.J. Basu, On self-sustained oscillations in two-dimensional compressible flow over rectangular cavities, *J. Fluid Mech.*, vol. 455, 2002, pp. 315-346.
[15] C.W. Rowley, T. Colonius, and R.M. Murray, Model reduction for compressible flows using POD and Galerkin projection, *Phys. D*, vol. 189, 2004, pp. 115-129.
[16] A. Balogh, W-J. Liu, M. Krstic, Stability enhancement by boundary control in 2D channel flow, *IEEE Transactions on Automatic Control*, vol. 46, 2001, pp 1696-1711.
[17] A. Balogh, O.M. Aamo, M. Krstic, Optimal mixing enhancement in 3-D pipe flow, *IEEE Transactions on Control Systems Technology*, vol. 13, 2005, pp 27-41.
[18] O.M. Aamo and M. Krstic, *Flow control by feedback*, Springer; 2003.
[19] O.M. Aamo, M. Krstic and T.R. Bewley, Control of mixing by boundary feedback in 2D channel flow, *Automatica*, vol. 39, 2003, pp 1597-1606.
[20] A.J. Chorin, J.E. Marsden, *A mathematical introduction to fluid mechanics*, Springer, 2000.
[21] www-math.mit.edu/˜seibold
[22] G. Besacon, H. Hammouri, On observe design for interconnected systems *Journal of Math. Systems, Estimation and Control*, vol. 8, 1998, pp 1-25.
[23] A. Isidori, *Nonlinear Control Systems*, Springer; 1994